

Design of a Compact Dual-Band Patch Antenna for ISM and 5G Use

Vignesh Kailash Boddu

Dept. of Electronics and Comm. Engg.

IIIT Nagpur

Nagpur, India

vigneshkailash1977@gmail.com

Venkata Sriram Vaibhav Bandaru

Dept. of Electronics and Comm. Engg.

IIIT Nagpur

Nagpur, India

bvsrvaibhav@gmail.com

Paritosh D.Peshwe

Dept. of Electronics and Comm. Engg.

IIIT Nagpur

Nagpur, India

paritoshpeshwe@gmail.com

Abstract—This paper presents a compact, dual-band, and flexible wearable antenna designed for modern wireless applications, specifically targeting the Industrial, Scientific, and Medical (ISM) band and the sub-6 GHz 5G NR band. The antenna operates effectively across two frequency ranges: 2.4442–2.5200 GHz and 3.6400–3.7652 GHz, and exhibits a low-profile geometry with dimensions of $40 \times 11.3 \times 3$ mm³. The structure is realized on a felt substrate characterized by a relative permittivity (ϵ_r) of 1.63 and a dielectric loss tangent ($\tan \delta$) of 0.044. A comprehensive parametric study was conducted to optimize performance parameters including impedance bandwidth, reflection coefficient, and gain. The proposed antenna achieves peak gains of 3.4287 dB and 4.1617 dB at 2.48 GHz and 3.71 GHz respectively, with well-defined 2D and 3D radiation characteristics. These results, combined with its compact and conformal profile, make the antenna a promising candidate for integration into wearable systems and emerging on-body communication technologies.

Index Terms—Wearable antenna, dual-band, ISM band, 5G NR, high-gain, flexible substrate, felt material.

I. INTRODUCTION

The evolution of wearable electronics has driven the need for advanced antenna systems that can support multiple wireless standards within compact and flexible form factors [1]. With applications expanding into biomedical sensing, personal communication, and body-centric data transmission, there is growing demand for antennas that operate efficiently over multiple frequency bands, especially within the ISM and sub-6 GHz 5G NR spectra [3]. Reliable performance in these scenarios requires antennas with dual-band functionality, low-profile structures, and mechanical flexibility [5]. Recent developments emphasize flexible dielectric substrates and optimized geometries to ensure stable electromagnetic performance [6]. Such design considerations are crucial for seamless integration into wearable platforms, enabling consistent radiation characteristics, low power loss, and robust connectivity in on-body environments [4].

The choice of substrate and conductive materials plays a pivotal role in wearable antenna suitability. Rigid substrates like FR4, though common in conventional designs, lack the flexibility needed for conforming to dynamic body surfaces, leading to discomfort and performance issues. Flexible substrates, by contrast, can endure bending and movement without compromising electromagnetic behavior [6].

Current research focuses on achieving compact, conformal, dual-band antennas for standards like the 2.45 GHz ISM band and sub-6 GHz 5G NR [3]. Techniques such as impedance matching with stubs, defected ground structures (DGS), and parasitic element coupling help enhance bandwidth and reduce reflection losses [5]. Additionally, the use of high-permittivity, low-loss flexible substrates enables stable performance under bending and stretching, maintaining consistent S_{11} and gain profiles in on-body scenarios [7]. These advancements aim to optimize radiation efficiency, minimize SAR levels, and ensure reliable operation under dynamic mechanical and environmental conditions.

A dual-band antenna utilizing a folded patch configuration has been reported in [8], targeting frequency ranges of 1.7–1.9 GHz and 2.4–2.5 GHz, making it suitable for general wireless communication systems. In [9], a compact on-chip antenna designed for 2.4 GHz and 5 GHz WLAN applications is presented.

This paper presents a high-performance, dual-band wearable antenna designed specifically for operation in the 2.45GHz ISM and sub-6GHz 5G NR frequency ranges. The antenna exhibits effective resonance across two targeted bands: 2.4442–2.5200 GHz and 3.6400–3.7652 GHz, making it suitable for low-power medical, industrial, and next-generation mobile communication applications [1]. The design utilizes a flexible felt substrate characterized by a relative permittivity (ϵ_r) of 1.63 and a dielectric loss tangent ($\tan \delta$) of 0.044, enabling excellent mechanical flexibility along with stable RF behavior. Despite its compact dimensions of $40 \times 11.3 \times 3$ mm³, the antenna achieves impressive peak gains of 3.4287 dB and 4.1617 dB at 2.48 GHz and 3.71 GHz.

II. ANTENNA DESIGN

The physical structure of the developed dual-band antenna is presented in Fig. 1, showcasing both front layout. The antenna is implemented on a soft felt substrate with a low relative permittivity (ϵ_r) of 1.63 and a dielectric loss tangent ($\tan \delta$) of 0.044, enabling both electrical stability and physical flexibility. The total profile thickness is 3mm, suitable for seamless integration into fabric-based or body-mounted platforms. A standard 50-ohm micro-strip feedline is used to excite the

radiating patch. The compact dimensions $40 \times 11.3 \times 3 \text{ mm}^3$ support miniaturization without sacrificing performance.

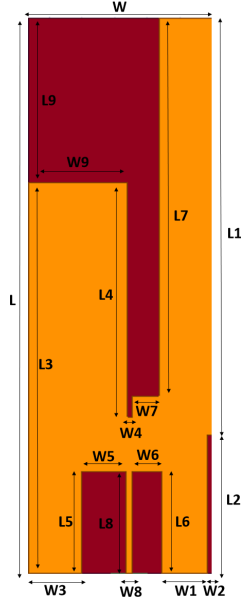


Fig. 1: Top View of the proposed dual-band antenna.

TABLE I: Parameters of Antenna

Parameter	Dim. (mm)	Parameter	Dim. (mm)
L	40	W	11.3
L1	30	W1	2.8
L2	10	W2	0.3
L3	28.2	W3	3.3
L4	15.4	W4	0.3
L5	7.36	W5	2.7
L6	7.36	W6	1.8
L7	27.2	W7	1.6
L8	7.36	W8	0.4
L9	11.8	W9	6.1

Using ANSYS, the antenna delivers dual-band resonance, covering 2.4442–2.5200 GHz and 3.6400–3.7652 GHz, aligning with ISM and 5G NR bands, respectively. It also achieves substantial peak gain values of 3.4287 dB and 4.1617 dB at 2.48 GHz and 3.71 GHz, indicating strong radiative efficiency and suitability for low-profile, body-centric wireless systems.

A. Design Evolution

As shown in Fig. 2, Iteration 1 modifies the antenna from [11], originally resonating at 2.45 GHz, by adding a top-edge cut that shifts the frequency to 3.3 GHz, though still single-band. Iteration 2 deepens the cut to form a longer notch, enhancing current flow and impedance matching, resulting in resonances at 2.8 GHz and 4.3 GHz with return losses of -28 dB and -21 dB. To further improve high-frequency response, Iteration 3 adds a vertical cut on one side, creating two current paths and achieving resonances at 2.5 GHz and 4.1 GHz with return losses of -13 dB and -16 dB. Finally, Iteration 4 optimizes the position and depth of both cuts, producing sharp resonances at 2.48 GHz and 3.8 GHz. These structural

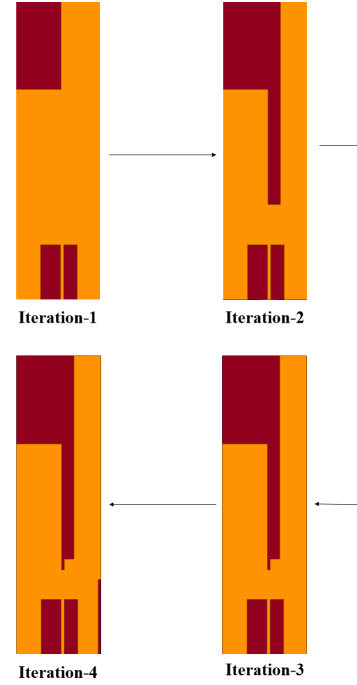


Fig. 2: Design Evolution

refinements enable stable dual-band operation across the ISM and sub-6 GHz 5G bands by improving impedance matching and radiation performance.

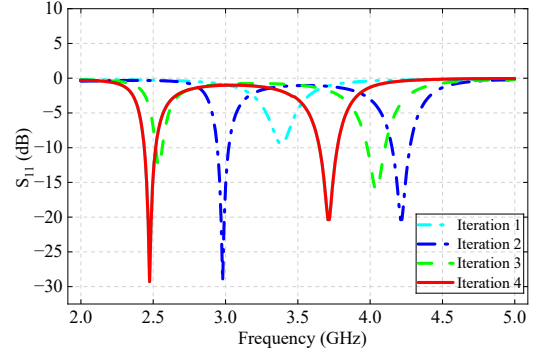


Fig. 3: S_{11} parameter for design evolution.

III. RESULTS AND ANALYSIS

The following section discusses Reflection Coefficient Analysis, Gain Analysis, Current Distribution, 2D/3D Radiation Pattern and Parametric Analysis of the antenna design.

A. Reflection Coefficient Analysis

The simulated reflection coefficient S_{11} response of the proposed dual-band antenna, as depicted in Figure 4 shows that the proposed dual-band antenna achieves good impedance matching at two key frequency bands. Clear resonance is observed at 2.48 GHz and 3.71 GHz with return loss values of -29.26 dB and -20.35 dB, indicating efficient radiation at

both ISM and sub-6 GHz 5G bands. The bandwidth covers slight frequency shifts caused by bending or fabric variations, which is vital for wearable use. These results confirm that the antenna effectively supports dual-band operation and is suitable for integration into flexible body-worn devices.

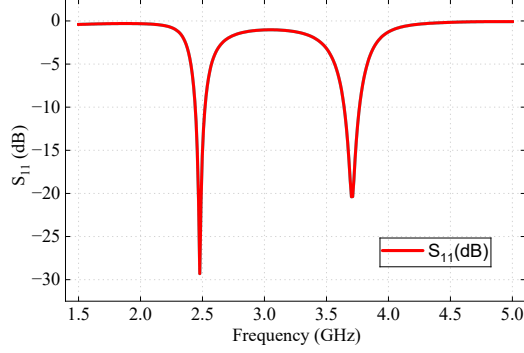


Fig. 4: Simulated reflection coefficient S_{11} of antenna.

B. Gain Analysis

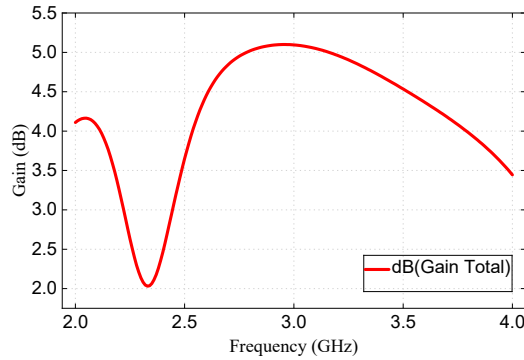


Fig. 5: Gain Total of the Dual Band Antenna

The simulated gain response of the proposed antenna, as depicted in Fig. 5, spans the 0–8 GHz frequency range. The antenna maintains a positive gain (above 0 dB) approximately between 0.9 GHz and 5.2 GHz, indicating efficient radiation across this broad operational band. Within this range, two distinct gain peaks are observed at 2.48 GHz and 3.71 GHz, achieving values of 3.43 dB and 4.16 dB, respectively.

C. Current Distribution

The simulation image represents the surface current density distribution (J_{surf}) in a planar electromagnetic structure, modeled using Ansys 2024 R2. As seen in Fig. 6, the color gradient map illustrates variations in surface current density ranging from 2.21 to 110 A/m. High current concentrations, indicated by red and dark red regions, are observed along the conducting paths, suggesting efficient current flow in these segments.

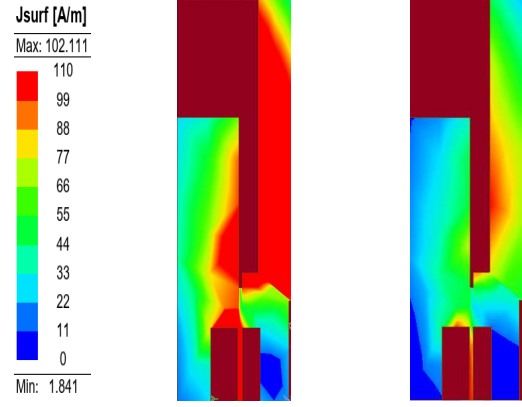
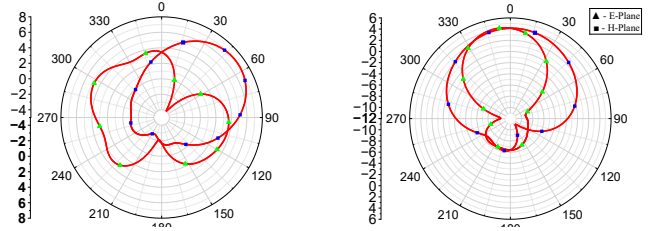


Fig. 6: Current distribution at 2.45 GHz and 3.8 GHz.

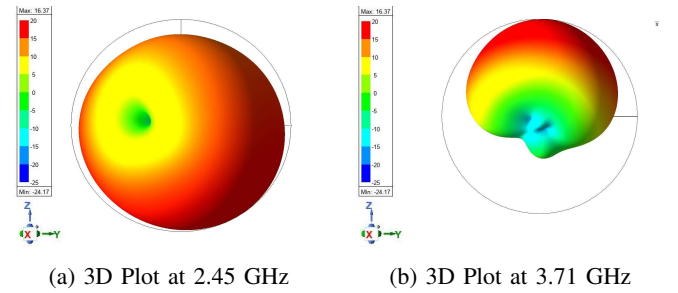
D. 2D/3D Radiation Pattern

Fig. 7 presents the 2D radiation patterns of the proposed antenna at 2.48 GHz for two principal planes: $\phi = 0^\circ$ and $\phi = 90^\circ$. The plot corresponding to $\phi = 0^\circ$ exhibits a bidirectional radiation pattern, characteristic of typical E-plane behavior, while the pattern for $\phi = 90^\circ$ shows an omnidirectional-like distribution resembling H-plane response.



(a) Radiation pattern at 2.45 GHz (b) Radiation pattern at 3.71 GHz

Fig. 7: Simulated far-field radiation patterns of the antenna at 2.45 GHz and 3.71 GHz in $\phi = 0^\circ$ and $\phi = 90^\circ$ planes.



(a) 3D Plot at 2.45 GHz (b) 3D Plot at 3.71 GHz

Fig. 8: 3-D Plots at 2.45 GHz and 3.71 GHz.

E. Bending Analysis

The plot shows curves for bending angles of 10° , 15° , and 30° . At 10° , the antenna has the strongest resonance dips at 2.45 GHz and 4 GHz, showing good impedance matching and low reflection. With greater bending, a slight drop in return loss appears, mainly at higher frequencies. This confirms

the antenna keeps stable dual-band performance under slight bending, making it fit for wearable use where steady operation during movement is needed.

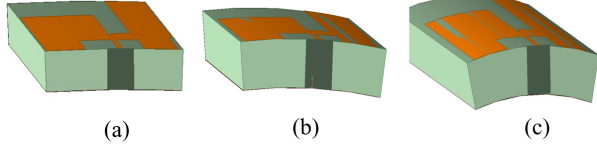


Fig. 9: Band Bending at 10°, 15°, and 30°

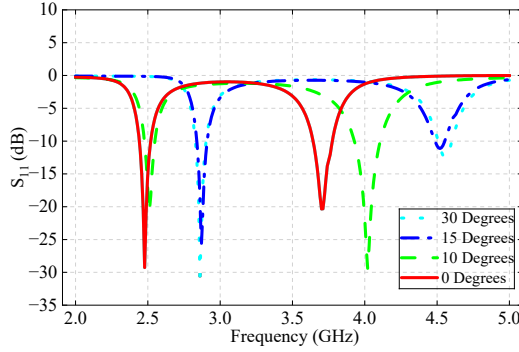


Fig. 10: S_{11} response at 10°, 15°, and 30°.

F. Specific Absorption Rate (SAR)

SAR quantifies how much RF energy is absorbed by body tissues and depends on tissue conductivity, electric field strength, and density [12]. According to FCC guidelines, SAR should not exceed 1.6 W/kg for 1 gram of tissue. In this study, the antenna's SAR was simulated using a three-layer tissue model with a 2 mm separation. As illustrated in Figure 11, the maximum SAR was found to be 0.483 W/kg, which is well within the regulatory limit, confirming that the design is safe for on-body use.

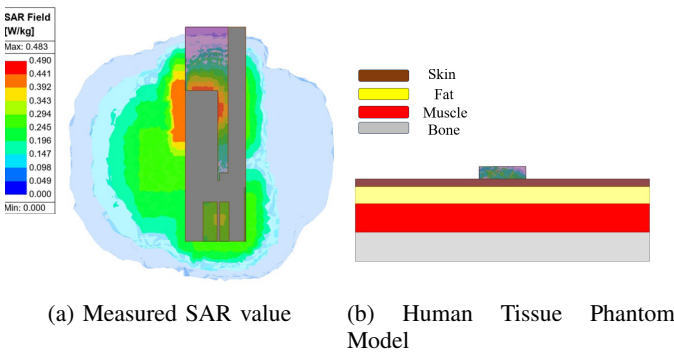


Fig. 11: SAR and Phantom Model

TABLE II: Properties of Human Phantom Model

Property	Skin	Fat	Muscle	Bone
Dielectric Constant (ϵ)	31.29	5.28	52.79	12.66
Conductivity σ (S/m)	1.46	0.10	1.705	0.38
Density ρ (kg/m ³)	1100	1100	1060	1850
Loss Tangent	0.26	0.04	0.24191	0.10
Thickness (mm)	2	4	7	7

TABLE III: Comparison with existing wearable antennas

Ref.	Size (mm ³)	Bands (GHz)	BW (%)	Gain (dB)
[4]	55 × 52 × 1.52	2.45	60	–
[6]	45 × 40 × 1.6	2.45	58	6.8
[8]	32 × 39 × 1.6	2.4 / 5	102	2
Proposed	40 × 11.3 × 3	2.45, 3.71	62.94	3.43 / 4.16

IV. CONCLUSION

This work presents a compact and flexible dual-band antenna demonstrates excellent potential for next-generation wearable and body-centric wireless systems. By leveraging a low-permittivity felt substrate and a ground structure, the design achieves stable impedance matching and efficient radiation within the 2.4 GHz ISM band and sub-6 GHz 5G NR range. Full-wave simulation results verify dual-band operation with peak gains of 3.4287 dB and 4.1617 dB at 2.48 GHz and 3.71 GHz, respectively. The antenna's low-profile form factor, robust performance, and conformal characteristics make it well-suited for seamless integration into smart textiles and on-body communication platforms, paving the way for reliable and unobtrusive wireless connectivity in wearable applications.

REFERENCES

- [1] G. A. Conway and W. G. Scanlon, "Antennas for Over-Body-Surface Communication at 2.45 GHz," *IEEE Trans. Antennas Propag.*, vol. 57, no. 4, pp. 844–855, Apr. 2009.
- [2] R. Salvado, C. Loss, R. Gonçalves, and P. Pinho, "Textile Materials for the Design of Wearable Antennas: A Survey," *Sensors*, vol. 12, no. 11, pp. 15841–15857, 2012.
- [3] M. K. A. Rahim et al., "Dual-Band Wearable Textile Antenna for Body-Centric Communications," *Progress In Electromagnetics Research*, vol. 138, pp. 485–498, 2013.
- [4] P. Salonen, Y. Rahmat-Samii, and M. Kivikoski, "Wearable Antennas in the Vicinity of Human Body," *IEEE Antennas and Propagation Magazine*, vol. 45, no. 2, pp. 97–107, Apr. 2003.
- [5] A. Tronquo, H. Rogier, C. Hertleer, and L. Van Langenhove, "Robust planar textile antenna for wireless body LANs operating in 2.45 GHz ISM band," *Electronics Letters*, vol. 42, no. 3, pp. 142–143, Feb. 2006.
- [6] H. Giddens et al., "Flexible Substrate Materials for Wearable Antennas," *IEEE Antennas Wireless Propag. Lett.*, vol. 14, pp. 1490–1493, 2015.
- [7] R. Chahat, M. Zhadobov, L. Le Coq, and R. Sauleau, "Wearable Endfire Textile Antenna for On-Body Communications at 60 GHz," *IEEE Antennas Wireless Propag. Lett.*, vol. 11, pp. 799–802, 2012.
- [8] C. Y. Chiu, C. C. Chan, and K. M. Luk, "Small dual-band antenna with folded-patch technique," *IEEE Antenna Wireless Propag. Lett.*, vol. 3, pp. 108–110, 2004.
- [9] S. Kim, S. Hong, J. Cho, and J. Kim, "A Dual-Band On-Chip Antenna for 2.4/5 GHz WLAN Applications," *Microwave and Optical Technology Letters*, vol. 53, no. 3, pp. 542–544, Mar. 2011.
- [10] P. Salonen and L. Hurme, "A novel fabric WLAN antenna for wearable applications," in *Proc. IEEE Antennas Propag. Soc. Int. Symp. Dig. Held Conjunct., USNC/CNC/URSI North Amer. Radio Sci. Meeting*, Mar. 2004.
- [11] A. Smida, A. Iqbal, A. J. Alazemi, M. I. Waly, R. Ghayoula, and S. Kim, "Wideband wearable antenna for biomedical telemetry applications," in *Proc. IEEE Int. Conf. on Computing, Electronics & Communications Engineering (icCECE)*, London, UK, Aug. 2018, pp. 95–99.

- [12] U. Ali, S. Ullah, J. Khan, M. Shafi, B. Kamal, A. Basir, J. A. Flint, and R. D. Seager, "Design and SAR Analysis of Wearable Antenna on Various Parts of Human Body Using Conventional and Artificial Ground Planes," *Journal of Electrical Engineering and Technology*, vol. 12, no. 1, pp. 317–328, Dec. 2016.